

Spreading of damage in the quantum $S = \frac{1}{2}$ Heisenberg ferromagnet

I. V. Rojdestvenski, M. L. Lyra, and U. M. S. Costa

Departamento de Física, Universidade Federal de Alagoas, Maceió AL 57072-970, Brazil

(Received 24 January 1997)

We suggest a tool to investigate the processes of the ferromagnetic ordering in the quantum Heisenberg model. We introduce the spreading of a damage technique based on the Handscomb Monte Carlo method and apply it to the three-dimensional simple cubic Heisenberg ferromagnet. Particularly, we study the thermal dependence of the *graph Hamming distance* and employ a finite-size scaling analysis of its size dependence. It is obtained that a properly defined Hamming distance displays a maximum at a characteristic temperature T_s , below which it becomes roughly size independent. We discuss the properties of these dependences in relevance to other thermodynamic functions of the model. [S0163-1829(97)02829-4]

I. INTRODUCTION

The Handscomb Monte Carlo method was introduced in 1962–1964 (Refs. 1 and 2) in a form applicable for the calculation of the thermodynamic properties of the $S = 1/2$ isotropic quantum Heisenberg ferromagnet. Since then, the technique has been generalized by many authors and proved itself to be a powerful tool for the investigation of the critical properties of quantum spin models.^{3–10} The main feature of this technique in comparison with the standard Metropolis technique is the fact that the sample space is not related to any kind of physical phase space. The Markov chain is constructed over the space of ordered Mayer diagrams and it is the diagrammatic series of the partition function that is calculated by means of the Monte Carlo method. Consequently, the set of probabilities utilized in the Handscomb technique has no relevant observable analogy, as the canonic Gibbs exponentials in the standard Monte Carlo.

In the past few years, the spreading of the damage technique has been widely used to study the critical properties of classical Ising-like systems.^{11–13} The concept of the spreading of the damage technique in general can be formulated as follows. At first we apply the Monte Carlo method to reach the thermal equilibrium at a given temperature. Then, we take the obtained equilibrium configuration and make an exact replica of it. After that, we introduce a *damage* into the replica, i.e., we modify it compared to the original configuration. For example, in the case of a standard Monte Carlo applied to the $S = 1/2$ Ising model, this alteration might be the flipping of one spin in the obtained equilibrium configuration. After the damage has been introduced, we initiate two synchronous Monte Carlo procedures, taking as the initial states the two configurations (modified replica and original). Both procedures are identical in the sense of using the same set of random numbers and transition probabilities.

The quantity that is calculated during the described process is the *Hamming distance*,¹⁵ which is the measure of how different both spin configurations become as time goes on. For the case of the Ising model the Hamming distance is the average relative number of lattice sites which have different values of the spin variables in both configurations, averaged along the Markov chain.

The Hamming distance displays a critical behavior at the

so-called critical spreading temperature T_s .^{11,12} Within the heat-bath dynamics and with a fixed damaged spin trick, it can be shown that T_s is the same as the Curie temperature T_C for Ising spin systems.¹⁴ However, results reported from simulations using Glauber and Metropolis algorithms indicate that T_s differs from T_C by several percent in $3d$ bulk systems,^{11,16} and that T_s is slightly smaller than T_C in two dimensions.¹⁷ It is worth mentioning that the thermal properties of the Hamming distance are strongly dependent on the type of dynamic rules used in the Monte Carlo process. When the Metropolis dynamics is used, a typical thermal dependence of the Hamming distance is a step function, which is equal to 0.5 above T_s and is zero below it. In the cases of Glauber and heat-bath dynamics, the behavior of the Hamming distance is different and is proved to be dependent on the way the damage is introduced.¹³ This is quite different from the usual statistical Monte Carlo modeling where all the dynamics give the same values for the magnetization, susceptibility, and specific heat, differing only in the convergence rate.¹⁸

It is a problem, however, to introduce a similar technique for a quantum Monte Carlo method. The main reason is the above-mentioned lack of the correspondence between the sample space of the Handscomb procedure and the physical phase space of the investigated system.

In this paper we introduce a spreading of the damage technique for the Handscomb Monte Carlo dynamics. In this technique the damage is introduced as a perturbation in the bond structure of the Mayer diagrams, which form the sample space for the Markov chain. In Sec. II, we discuss the Handscomb algorithm in the view of the possible ways to introduce the damage and to define the Hamming distance. In Sec. III we present the results of our simulations for the three-dimensional simple cubic Heisenberg ferromagnet and discuss the thermal and size dependences of the Hamming distance in comparison with other thermal properties. In the conclusions, we make a brief summary of our results and sketch the prospectives of our approach.

II. THE HANDSCOMB MONTE CARLO DYNAMICS

Before introducing the spreading of damage technique for the Handscomb Monte Carlo method it is worth sketching

the Handscomb method itself and discuss its internal dynamics.

Let the Hamiltonian of the system to be represented in the following form:

$$H = \sum_i^{N_0} H_i, \quad [H_i, H_j] \neq 0, \quad (1)$$

where $[A, B] = AB - BA$, with N_0 being the total number of bonds in the system. For example, we write the Heisenberg Hamiltonian in the absence of applied magnetic field as

$$H = -2 \sum_{(i,j)} J_{i,j} S_i S_j, \quad (2)$$

Then, for the canonic average of any physical observable A , we can write

$$\begin{aligned} \langle A \rangle &= \frac{\text{Tr}(A e^{-\beta H})}{\text{Tr}(e^{-\beta H})} = \frac{\sum_r \sum_{C_r} [(-\beta)^r / r!] \text{Tr}[A H_{i_1} \dots H_{i_r}]}{\sum_r \sum_{C_r} [(-\beta)^r / r!] \text{Tr}[H_{i_1} \dots H_{i_r}]} \\ &= \sum_r \sum_{C_r} A(C_r) p(C_r), \end{aligned} \quad (3)$$

where $\beta = 1/k_B T$, \sum_{C_r} denotes the summation over all ordered r element sets of indices $C_r = \{i_1, \dots, i_r\}$ (Mayer diagrams) and

$$A(C_r) = \frac{\text{Tr}[A H_{i_1} \dots H_{i_r}]}{\text{Tr}[H_{i_1} \dots H_{i_r}]}, \quad (4)$$

$$p(C_r) = \frac{[(-\beta)^r / r!] \text{Tr}[H_{i_1} \dots H_{i_r}]}{\sum_r \sum_{C_r} [(-\beta)^r / r!] \text{Tr}[H_{i_1} \dots H_{i_r}]} \quad (5)$$

Formally, if $p(C_r) \geq 0$, we can consider it as a probability distribution and write for the canonical average:

$$\langle A \rangle_{\text{canonic}} = \langle A(C_r) \rangle_{p(C_r)}. \quad (6)$$

The essence of the Handscomb Monte Carlo method is in organizing a random walk in the space of the diagrams C_r with the limit distribution of the Markov chain being $p(C_r)$.

When we apply the above general scheme to the $S = 1/2$ Heisenberg model, we reformulate the Hamiltonian in the well-known representation of the transposition operators as follows:

$$H = - \sum J_{i,j} E_{i,j} + \text{const}, \quad (7)$$

where $E_{i,j}$ is a transposition operator which exchanges the spin variables between sites i and j . Then $H_i = -J_{t_1, t'_1} E_{t_1, t'_1}$ and

$$P(C_r) = H_{i_1} \dots H_{i_r} \quad (8)$$

is a permutation operator. Now we are able to calculate the necessary traces in Eq. (6) exactly. For every given diagram C_r the contribution is given by

$$\text{Tr}_{C_r} = \text{Tr}(H_{i_1} \dots H_{i_r}) = \left[\prod_{j=1}^r J_{t_j, t'_j} \right] 2^{k(C_r)}, \quad (9)$$

where $k(C_r)$ is the number of cycles in the permutation $P(C_r)$.

The random-walk dynamics suggested by Handscomb consists of three types of steps:

(1) Step *forward*, which increases the number of bonds r in the diagram C_r , adding a randomly chosen bond from the left:

$$C_r \rightarrow C_r i. \quad (10)$$

(2) Step *backwards*, which decreases the number of bonds, taking out one bond from the right:

$$C_r = j C_{r-1} \rightarrow C_{r-1}. \quad (11)$$

(3) The *cyclic transposition*, or the movement of one bond from right to the left:

$$C_r = j C_{r-1} \rightarrow C_{r-1} j = C'_r. \quad (12)$$

We should stress that, because of noncommutativity of the H_i elements, the last process is nontrivial, though the trace remains unaltered. As well, we introduce the probability of the choice of the *forward* step f_r ($0 < f_r < 1$) and the probability $p(i)$ of a random choice of the included bond [$\sum_i p(i) = 1$].

Once an initial configuration C_r is given, the realization of the above steps in the stochastic procedure is constructed as follows: At first, we choose step *forward* with probability f_r [step *backwards* is then chosen with probability $(1 - f_r)$]. If the step *forward* is chosen, then we choose the bond i with probability $p(i)$, and with the transition probability $T^+(C_r, C_r i)$ we accept $C_r i$ as a new state. Otherwise the state remains unchanged. If a *backwards* step is chosen, we perform the transition (11) with probability $T^-(i C_{r-1}, C_{r-1})$, otherwise we accomplish the *cyclic transposition*. The functions T^+ and T^- are defined as follows:

$$T^+(C_r, C_r i) = \min \left[1, \frac{\beta(1 - f_{r+1}) \text{Tr}_{i C_r}}{(r+1) f_r p(i) \text{Tr}_{C_r}} \right], \quad (13)$$

$$T^-(i C_{r-1}, C_{r-1}) = \min \left[1, \frac{r f_{r-1} p(i) \text{Tr}_{C_{r-1}}}{\beta(1 - f_r) \text{Tr}_{C_r}} \right]. \quad (14)$$

In practice, it is enough to chose the distributions $p(i)$ and f_r as follows:²⁰

$$p(i) = \frac{1}{N_0}, \quad f_r = (1 + \delta_{r,0})/2, \quad (15)$$

where $\delta_{r,0}$ is the usual delta function.

The random variables for the thermodynamic parameters can be devised using Eq. (5) for $A(C_r)$, taking for A the operators of different physical variables. For example, for the internal energy we have²

$$E = \langle H \rangle = - \left\langle \frac{r}{\beta} \right\rangle + \text{const}. \quad (16)$$

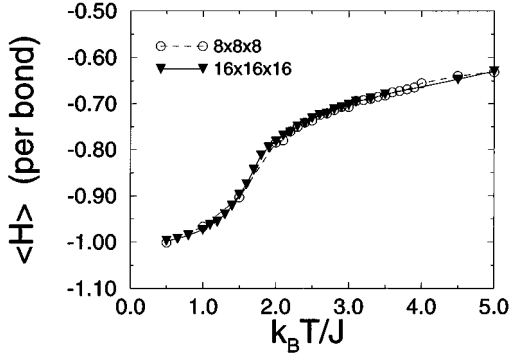


FIG. 1. The thermal dependence of the internal energy per bond (in units of J) for the simple cubic Heisenberg magnet $S=1/2$, as obtained in our simulations using the Handscomb Monte Carlo method.

We should note here that there is a general analogy of the sample space for the canonic distribution in the Handscomb approach with a grand canonic distribution in some artificial chain polymer model, with the number of bonds r in C_r playing the role of the number of particles. In this sense, Eq. (16) for the internal energy appears to describe the average number of particles in this artificial polymer system.

The characteristic feature of the dynamics described above is that it provides for a very intensive mixing of the states of the sample space. This is due to two facts. Besides the transition probabilities being sufficiently high for any kind of steps, the step *forward* is accomplished on the right edge of C_r while the step *backwards* is attempted from the left side. This makes the procedure microscopically irreversible, thus increasing the mixing. However, this microscopic irreversibility satisfies the generalized detailed balance principle.^{1,20}

The results of the calculation of the internal energy for a simple cubic Heisenberg ferromagnet by means of the Handscomb method are presented in Fig. 1. We have studied systems of $4 \times 4 \times 4$ up to $32 \times 32 \times 32$ spins. The length of the Markov chains were about 1000 MC steps/spin, with about 300 MC steps/spin left for the thermal relaxation.

To discuss the spreading of damage phenomenon it is worth evaluating the Curie temperature by means of the same technique. We accomplished this by numerical differentiation of the internal energy with respect to temperature to obtain the specific heat and to find the position of its maximum (see Fig. 2). The estimated Curie temperature appeared to be $k_B T/J = 1.60 \pm 0.05$, which agrees reasonably with the data of Ref. 19, namely $k_B T/J = 1.68 \pm 0.01$.

III. SPREADING OF DAMAGE IN HANDSCOMB DYNAMICS

To introduce the spreading of damage technique for the described dynamics, we have to analyze the elements of the sample space, i.e., the diagrams C_r . We can describe three characteristics of C_r which describe it completely:

- (i) The total number of bonds r ;
- (ii) The abundance of different bonds in C_r ;
- (iii) The cyclic structure of the resulting permutation $P(C_r)$.

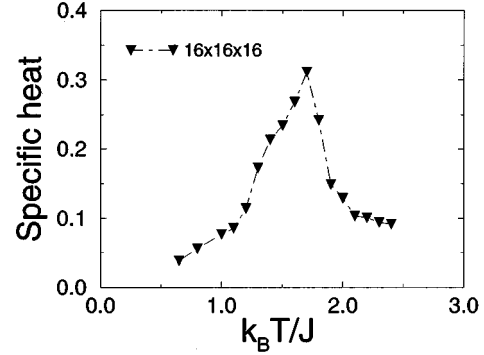


FIG. 2. The thermal dependence of the specific heat per bond (in units of k_B). The points were obtained from numerical differentiation of the internal energy thermal dependence for lattices of $16 \times 16 \times 16$ sites.

We should note here that the first two characteristics are the same as they would be for a classical model treated by means of the Handscomb method, while in the third one the operator features of $P(C_r)$ are accounted for. If, for example, we make a permutation of different elements of C_r , the bond abundance and the total number of bonds will not change, while the changes in the cyclic structure might be significant due to the noncommutativity of different parts of the Hamiltonian.

In this paper we discuss the spreading of damage technique based on the bond abundance in C_r . The algorithm applied is as follows:

- (1) We set a Handscomb Monte Carlo procedure at a certain temperature and allow some time for the thermal relaxation to equilibrium.
- (2) We duplicate the equilibrium C_r and alter one bond in the replica.
- (3) We apply the Handscomb procedure simultaneously to both configurations, using the same set of random numbers and attempting to introduce exactly the same bonds ($t_1 t'_1$) when making the step *forward*.

The principal moment of the technique is to introduce adequately the Hamming distance. Firstly, we attempted to construct it as follows:

$$D_a = \left\langle \frac{1}{N_0} \sum_{i=1}^{N_0} (n_i^{(1)} - n_i^{(2)})^2 \right\rangle, \quad (17)$$

where the quantity $n_i^{(1)}$ is the number of bonds i in the C_r and $n_i^{(2)}$ is the same for the replica. We call Eq. (17) the definition of the *absolute Hamming distance*.

The thermal dependence of D_a is presented in Fig. 3 for the system sizes $8 \times 8 \times 8$ and $16 \times 16 \times 16$. The main features of the presented curves are the following. Contrary to the spreading of damage in classical Ising-like systems, no peculiar behavior is observed in the vicinity of the critical point. The curves are monotonically decreasing with the increase of temperature. Another characteristic feature is that the absolute Hamming distance displays a strong size dependence, which is stronger at low temperatures. Its displayed finite (although small) values are probably due to the above-mentioned intensive mixing of states. The numerical data indicates that, after a sufficiently long time, D_a shall vanish

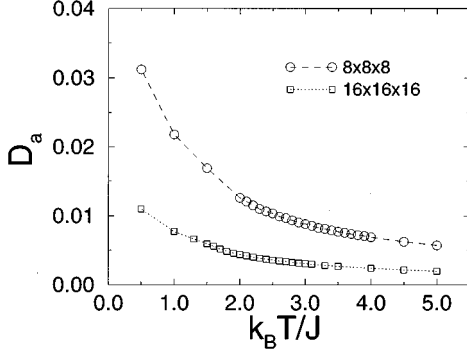


FIG. 3. The absolute Hamming distance vs temperature. Notice a tendency to vanishing in the thermodynamic limit for all temperatures.

in the thermodynamical limit for all temperatures. Therefore, both C_r and its replica exhibit in equilibrium the same average bond abundance.

However, the difference in the bond abundance itself is not sufficient to completely characterize the degree of likelihood of two diagram configurations, once they can also differ in the total number of bonds as well as on their proper cycle structure. In order to take the first of these possibilities into account when computing the damage spreading, we introduce another definition of the Hamming distance, which we call the *relative Hamming distance*:

$$D_r = \left\langle \sum_{i=1}^{N_0} \left| \frac{n_i^{(1)}}{r^{(1)}} - \frac{n_i^{(2)}}{r^{(2)}} \right| \right\rangle, \quad (18)$$

the numbers $r^{(1)}$ and $r^{(2)}$ being, respectively, the total number of bonds in C_r and its replica. In practice, we are taking into account the fact that the replica and the original configurations start to have different lengths as the Markov process evolves. By using the above definition, we are normalizing the bond abundance n_i to the total number of bonds r of each diagram, and comparing just relative quantities. In this way, we can distinguish diagram configurations which exhibit the same bond abundance but distinct lengths.

The thermal dependence of the relative Hamming distance is displayed in Fig. 4 for systems of different sizes. The characteristic feature of this dependence is that it displays a

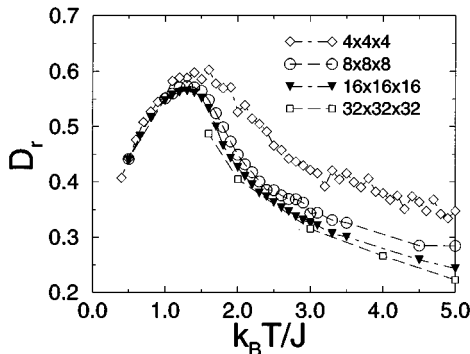


FIG. 4. The relative Hamming distance vs temperature. Notice that it becomes roughly size independent below a characteristic temperature $T_s < T_c$.

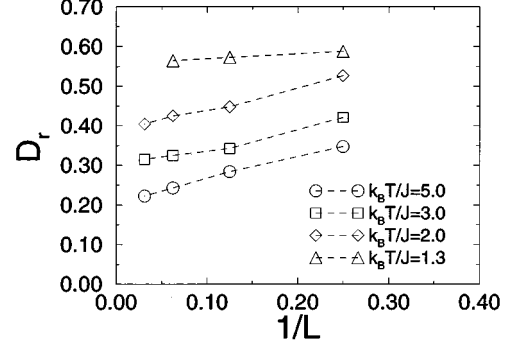


FIG. 5. The size dependence of the relative Hamming distance. It is roughly size independent for $T < T_s$, with $k_B T/J \approx 1.3$. Extrapolation of the numerical results for the limit $L \rightarrow \infty$ indicates that D_r vanishes for $T \rightarrow \infty$, but remains finite for finite temperatures.

pronounced maximum at a temperature around $k_B T/J = 1.3$, the height of which depends on the size of the system very weakly. We can associate this peak with some sort of a characteristic spreading temperature $T_s < T_c$.

Another interesting feature of the data in Fig. 4 is that for temperatures higher than T_s the smaller the system, the greater the relative Hamming distance. As a possible explanation for this phenomenon, we can argue that, when the temperature is high enough, the cyclic structure in the permutations (or, in other words, the cluster structure on the lattice) affects weakly the transition probabilities. Then, in a first approximation one can neglect its influence and therefore the choice of bonds becomes random with a uniform probability distribution. Only the total number of bonds r is determined by the temperature and N_0 . In this case $\langle r \rangle \approx N_0$, which causes the discussed behavior of the relative Hamming distance.

The above arguments can be illustrated by a finite-size scaling analysis (see Fig. 5). The data on this figure suggest that the closer the temperature is to T_s , the weaker the size dependence of the relative Hamming distance becomes. This happens, probably, due to the greater influence of the cyclic structure on the dynamics in the vicinity and below T_s . Indeed, at low temperatures the dominant distinction among equilibrium diagram configurations shall be on their cycle structure, which explain the fact that $D_r(T \rightarrow 0) \rightarrow 0$. The shapes of the size dependences of the relative Hamming distance display a tendency to saturation. However, the higher the temperature is, the slower this saturation appears to be. The crossover to size-independent behavior takes place at T_s , while the arguments above rule out the saturation in the limit of very high temperatures. Therefore, we can distinguish two dynamical regimes. For $T \gg T_s$ the dynamics is dominated by the bond abundance on the diagram configurations, whereas the cycle structure of the permutations becomes the relevant feature for $T \ll T_s$. The fact that the observed characteristic spreading temperature is smaller than the Curie temperature reflects the inability of the so defined relative Hamming distance in distinguishing the cycle structure of the diagrams.

IV. CONCLUSIONS

In the present paper we introduced a possible way of application of the spreading of damage technique to the Hand-

scomb Monte Carlo dynamics. We chose as an example the $S=1/2$ quantum Heisenberg ferromagnet on a simple cubic lattice. We showed that, for an appropriately defined analog for the Hamming distance, named the *relative Hamming distance*, there is a characteristic temperature at which the damage spreading is maximal, being roughly size independent at lower temperatures.

We should point out here that there might be another, perhaps, more physical way to introduce damage for this quantum Monte Carlo dynamics. If we define the Hamming distance as a measure of the difference in the cycle structure of the diagrams, we might be able to achieve a relation between the spreading properties and the magnetic ordering in the lattice. As well, when we investigate the spreading of damage in the bond abundance only, in some sense we are

studying classical characteristics of the diagrams, as it was discussed before. The cyclic structure may provide us with an insight to the quantization effects on the damage spreading. Work in this direction would certainly be valuable. Furthermore, it would be interesting to seek an explanation for the displayed size dependence of the relative Hamming distance.

ACKNOWLEDGMENTS

This work was partially supported by CNPq and FINEP (Brazilian research agencies). I.V.R. would like to acknowledge the kind hospitality of the Physics Department of UFAL and the FAPEAL agency (Alagoas, Brazil) for financial support of this study.

-
- ¹D. C. Handscomb, Proc. Camb. Philos. Soc. **58**, 594 (1962).
²D. C. Handscomb, Proc. Camb. Philos. Soc. **60**, 115 (1962).
³S. Chakravarty and D. B. Stein, Phys. Rev. Lett. **49**, 582 (1982).
⁴D. H. Lee, J. D. Joannopoulos, and J. W. Negele, Phys. Rev. B **30**, 1599 (1984).
⁵E. Manousakis and R. Salvador, Phys. Rev. B **39**, 575 (1989).
⁶G. Gomez-Santos, J. D. Joannopoulos, and J. W. Negele, Phys. Rev. B **39**, 4435 (1989).
⁷S. Kadowaki and A. Ueda, Prog. Theor. Phys. **82**, 493 (1989).
⁸A. W. Sandvik and J. Kurkijarvi, Phys. Rev. B **43**, 5950 (1990).
⁹T. V. Kuznetsova and P. N. Vorontsov-Velyaminov, J. Phys. Condens. Matter **5**, 717 (1993).
¹⁰I. V. Rojdestvenski and I. A. Favorsky, J. Phys. Condens. Matter **5**, L279 (1993).
¹¹U. M. S. Costa, J. Phys. A **20**, L583 (1987).
¹²H. E. Stanley, D. Stauffer, J. Kertész, and H. J. Herrmann, Phys. Rev. Lett. **59**, 2326 (1987).
¹³For a review see, e.g., N. Jan and L. de Arcangelis, in *Annual Reviews of Computational Physics*, edited by D. Stauffer (World Scientific, Singapore, 1994), Vol. 1, p. 1.
¹⁴A. Coniglio, L. de Arcangelis, H. J. Herrmann, and N. Jan, Europhys. Lett. **8**, 315 (1989).
¹⁵S. A. Kauffmann, J. Theor. Biol. **22**, 437 (1969).
¹⁶G. Le Caër, Physica A **159**, 329 (1989).
¹⁷P. Grassberg, J. Phys. A **28**, L67 (1995).
¹⁸B. Derrida and G. Weisbuch, Europhys. Lett. **4**, 657 (1987).
¹⁹G. S. Rushbrook, G. A. Baker, Jr., and P. J. Wood, in *Phase Transitions and Critical Phenomena*, edited by C. Domb and M. S. Green (Academic, New York, 1974), p. 245.
²⁰J. W. Lyklema, Phys. Rev. Lett. **49**, 88 (1982).